Front and domain growth in the presence of gravity

A. M. Lacasta
Departament de Física Aplicada, Universitat Politècnica de Catalunya, Jordi Girona Salgado 31, E-08034 Barcelona, Spain and Departament d'Estructura i Constituents de la Matèria, Universitat de Barcelona, Av. Diagonal 647, E-08028 Barcelona, Spain

A. Hernández-Machado and J. M. Sancho
Departament d'Estructura i Constituents de la Matèria, Universitat de Barcelona, Av. Diagonal 647, E-08028 Barcelona, Spain

(Received 23 April 1993)

Front and domain growth of a binary mixture in the presence of a gravitational field is studied. The interplay of bulk- and surface-diffusion mechanisms is analyzed. An equation for the evolution of interfaces is derived from a time-dependent Ginzburg-Landau equation with a concentration-dependent diffusion coefficient. Scaling arguments on this equation give the exponents of a power-law growth. Numerical integrations of the Ginzburg-Landau equation corroborate the theoretical analysis.

I. INTRODUCTION

Phase separation could be considered a prototype process in the study of domain growth and pattern formation in nonequilibrium phenomena.[1] A simple example is spinodal decomposition of binary mixtures. The system, which is initially in a homogeneous state, is suddenly quenched inside the coexistence region. At early times the presence of small fluctuations moves the system from the homogeneous state to a new one composed of domains of the new equilibrium phases. At late stages a convoluted interface separating the two new phases is formed. The main physical aspects of the evolution are now well understood. At long times the structures manifest spatiotemporal scaling described by a characteristic length, $R(t)$, which measures the average domain size. This quantity increases with a power law $R(t) \sim t^{\alpha}$ with $\alpha = \frac{1}{3}$ in accordance with Lifshitz-Slyozov theory.

The study of this nonequilibrium phenomenon when an external field is present is under active research.[2-8] Here, we study spinodal decomposition in a two-dimensional lattice in the presence of a constant gravitational field. Our model is a generalization[2,3] of model B of phase separation dynamics.[1] This generalized Ginzburg-Landau equation contains a concentration-dependent diffusion coefficient. In this way, the gravitational field appears not only through the closed boundary conditions but also in the dynamic equation.[2,3] Another situation that requires the hypothesis of a concentration-dependent diffusion coefficient appears in the modeling of deep quench in spinodal decomposition.[9-15]

Typical evolutions of the patterns for critical and off-critical quenches in the presence of gravity are presented in Figs. 1 and 2. From the initial uniform distribution to the final two-phase equilibrium state the evolution proceeds as follows: In the early stages domains are formed through the system, and they grow as in the absence of the external field. For longer times and large enough systems, these domains are affected by gravity, becoming elongated in the direction of the field. This process has been studied in detail in Refs. 5 and 6 for a system with periodic boundary conditions. As we observe in Fig. 1, apart from the domain growth, a different aspect is related to the presence of closed boundary conditions. In this situation, the field induces one of the phases (the more dense) to accumulate at the bottom and the other phase (the less dense) to accumulate at the top, giving rise to the growth of one layer at each of the boundaries. In this paper, we concentrate on the growth properties of these fronts of accumulated material. However, the domain growth in the bulk could be studied using a similar procedure. To characterize the different mechanisms acting during their evolution, we have studied analytically the dynamic equation of the fronts. This equation is derived from the generalized Ginzburg-Landau equation by using projection operator techniques.[13-17] A scaling analysis of the different terms of this equation determines the existence of power-law behavior for the thickness, $h(t) \sim t^{\alpha}$, with different growth exponents α. Apart from the characteristic exponent $\alpha = \frac{1}{3}$ of the Lifshitz-Slyosov theory related to a bulk diffusion mechanisms and the exponent $\alpha = \frac{1}{4}$ associated to a surface diffusion mechanisms induced by the concentration-dependent diffusion coefficient,[14] we obtain two other exponents ($\alpha = 1$ and $\alpha = \frac{1}{2}$) absent without gravity. The exponent $\alpha = 1$ is related to bulk diffusion as is expected from a simple linear growth which corresponds to a constant flux due to the presence of gravity. Furthermore, an exponent $\alpha = \frac{1}{2}$ is also obtained as the result of the crossed effects of a concentration-dependent diffusion coefficient and gravity. This exponent is related to a surface diffusion mechanism. At long times the $\alpha = 1$ exponent is dominant. However, for intermediate times a crossover from $\alpha = \frac{1}{2}$ to $\alpha = 1$ would be expected. The crossover

appears at a longer time for lower temperatures and at infinite time for zero temperature. Numerical integrations of the Ginzburg-Landau equation have been performed to corroborate the theoretical predictions for the front growth with fixed boundary conditions. Furthermore, we have also performed simulations for both fixed and periodic boundary conditions to characterize the domain growth in the bulk. Our results agree with an exponent $\alpha = 1$ in the long time behavior for finite temperature and $\alpha = \frac{1}{2}$ for zero temperature.

In Sec. II we introduce the theoretical model and the relevant quantities. In Sec. III the analysis of the interfacial equation is presented. The numerical integration and the corresponding results are discussed in Sec. IV. The final conclusions are given in Sec. V. Appendix A is devoted to mathematical details of the interfacial equation, and in Appendix B we give some details about the numerical integration.

II. THE MODEL

Our starting model is a generalization[2,3] of model B of phase separation dynamics:[1]

$$\frac{\partial}{\partial \tau}\bar{c}(\mathbf{r},\tau) = \nabla\Gamma(\bar{c})\cdot\nabla\frac{\delta F(\{\bar{c}\})}{\delta \bar{c}}, \tag{2.1}$$

where the coarse-grained free-energy functional $F(\{\bar{c}\})$

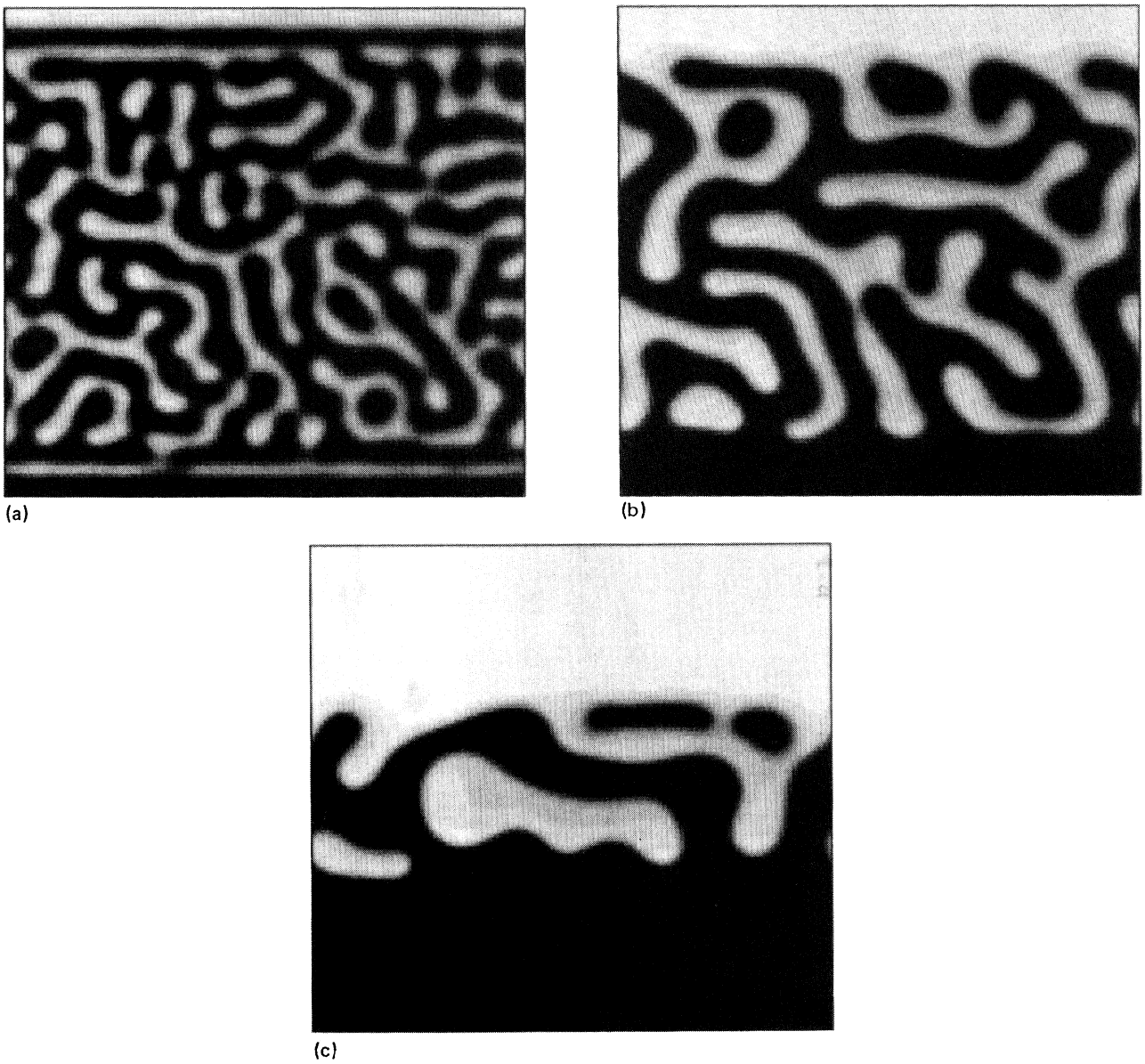

FIG. 1. Typical temporal evolution of phase separation for a critical quench in the presence of gravity, with $g = 0.1$ and $a = 0.8$. The figures correspond to the times (a) t=100, (b) t=500, and (c) t=2000.

contains the usual terms of the Ginzburg-Landau model plus the energy associated with a constant gravitational field in the $\hat{z}$ direction:

$$F(\{\bar{c}\}) = \int d\mathbf{r}' \left(-\frac{r}{2}\bar{c}^2 + \frac{u\bar{c}^4}{4} + \frac{k}{2}(\nabla\bar{c})^2 - Gz'\bar{c} \right), \quad (2.2)$$

r, u and k are phenomenological positive constants and G is the acceleration of gravity. $\Gamma(\bar{c})$ is the concentration-dependent diffusion coefficient:[2,3]

$$\Gamma(\bar{c}) = \Gamma_0(\bar{c}_0^2 - \bar{c}^2), \quad (2.3)$$

where Γ_0 is a constant, $\bar{c}_0 = \bar{c}_{st}(T = 0)$, and $\bar{c}_{st}(T)$ is the equilibrium concentration value for temperature T.

From Eqs. (2.1) and (2.2), a new equilibrium solution different from the one in the absence of gravity only appears through the effect of the appropiate boundary conditions. Regarding the dynamic evolution, the effect of the gravitational field through the boundary conditions in a finite system becomes less and less important as the system size increases. Then, the introduction of the dependence of $\Gamma(\bar{c})$ on $\bar{c}$ as given by Eq. (2.3), is required to provide an effect of the gravitational field in the dynamic evolution given by Eq. (2.1). It is simple to check that the gravitational contribution in the free energy, Eq. (2.2), disappears when Eq. (2.2) is inserted in the dynamical equation (2.1) if a constant diffusion coefficient hypothesis is considered. Here we consider the

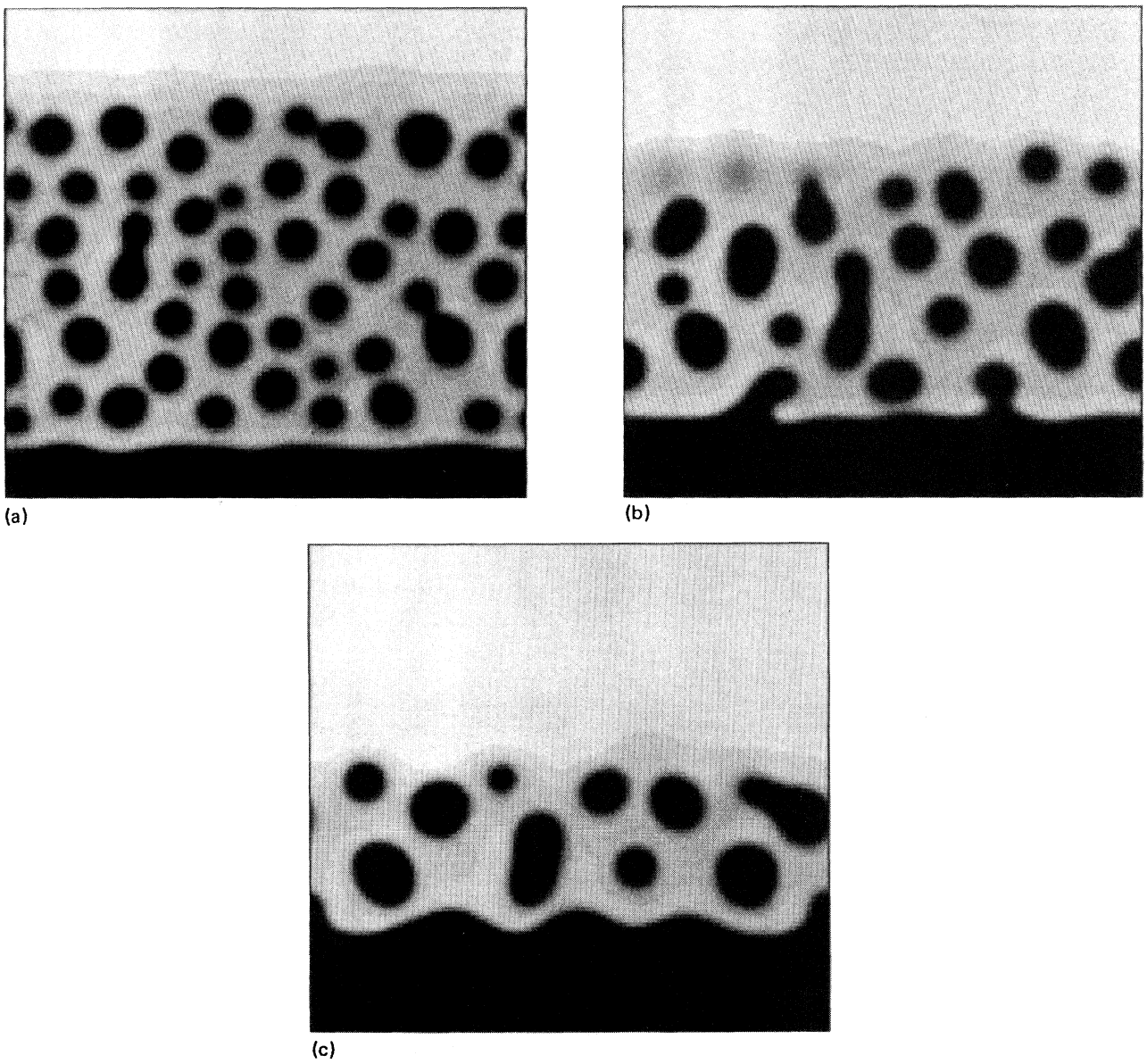

FIG. 2. Typical evolution for an off-critical quench that corresponds to a volume fraction of the minority phase $\phi = 30\%$, in the presence of gravity, with g=0.1 and a=0.8. The figures correspond to the times (a) t=500, (b) t=1000, and (c) t=1500.

effect of gravity both through boundary conditions and through the dynamic equation.

We assume periodic boundary conditions in the $\hat{x}$ direction perpendicular to the field and reflecting boundary conditions in the $\hat{z}$ direction parallel to the field. Equation (2.1) with Eq. (2.3) could be written in dimensionless form as

$$\frac{\partial c}{\partial t} = \boldsymbol{\nabla}(1 - ac^2) \cdot \boldsymbol{\nabla}(-c + c^3 - \boldsymbol{\nabla}^2 c - gz) \tag{2.4}$$

with

$$\mathbf{r} = \left(\frac{r}{k}\right)^{1/2} \mathbf{r}' \ , \quad t = \left(\frac{\Gamma_0 r^2 c_0^2}{k}\right) \tau \ , \quad c = \left(\frac{u}{r}\right)^{1/2} \bar{c} \ ,$$

$$g = \frac{(uk)^{1/2}}{r^2} G \ , \quad a = \left(\frac{\bar{c}_{st}(T)}{\bar{c}_0}\right)^2 \ . \tag{2.5}$$

The parameter a goes from 0 to 1 as temperature is reduced, and a=1 for T=0. The equilibrium concentration profile, c_{st}, in the presence of gravity obeys the following equation:[4]

$$-c_{st}(z) + c_{st}(z)^3 - \frac{d^2 c_{st}}{dz^2} = -gz. \tag{2.6}$$

If the gravitational field is very weak a perturbative expansion in g gives an approximate solution of Eq. (2.6) as

$$c_{st}(z) \sim c_0(z) + c_1(z) g, \tag{2.7}$$

where $c_0(z)$ is the unidimensional solution in absence of gravity

$$c_0(z) = \tanh\left(\frac{z}{\sqrt{2}}\right) \tag{2.8}$$

and $c_1(z)$ is given by[4]

$$c_1(z) = -\sqrt{2}\pi \tanh\left(\frac{z}{\sqrt{2}}\right) \operatorname{sech}\left(\frac{z}{\sqrt{2}}\right) - \frac{z}{8}\left[1 + 10\tanh^2\left(\frac{z}{\sqrt{2}}\right) - 7\tanh^4\left(\frac{z}{\sqrt{2}}\right)\right]. \tag{2.9}$$

In what follows, we will check the equilibrium profile given by Eq. (2.7), by numerical integration of Eq. (2.4). Furthermore, this profile will be used in our interfacial analysis.

III. INTERFACIAL THEORETICAL ANALYSIS

In Appendix A we derive an equation of evolution for the interface which separates the layer of accumulated material from the bulk in which spinodal decomposition takes place. By introducing a system of curvilinear coordinates (u, s) such that s follows the contour of the interface and u goes along the normal direction of it, we obtain the equation for the normal velocity $v(s,t)$:

$$4v(s,t) = (1-a)\int ds' W[\mathbf{r}(s), \mathbf{r}(s')]\,[\sigma K(s') + 2gZ(s')] + 4a\boldsymbol{\nabla}^2 K(s) - 4ag\cos\theta(s) K(s), \tag{3.1}$$

where $K(s)$ is the local curvature, σ is the surface tension, $Z(s)$ is the height of the interface, $\theta(s)$ is the angle between the normal to the interface and the direction of the gravitational field and $W(\mathbf{r}, \mathbf{r}')$ is the inverse of the Green function solution of Eq. (A9):[13]

$$\int ds'' G[\mathbf{r}(s), \mathbf{r}(s'')] W[\mathbf{r}(s''), \mathbf{r}(s')] = \delta(s - s'). \tag{3.2}$$

The first and second terms on the right-hand side of Eq. (3.1) represent the effects of surface tension and gravitational energy in the growth of the interface, respectively. The third and fourth terms only appear when a concentration-dependent diffusion coefficient is included ($a \neq 0$). Scaling analysis is now performed to obtain the exponents of the power laws associated with each term of Eq. (3.1), and the interpretation of the different mechanism associated with them. By rescaling the spatial variables with R and the time variables with $R^{1/\alpha}$, we see that

$$v \longrightarrow R^{1-1/\alpha} v \tag{3.3}$$

and then the characteristic growth exponents of the four terms in Eq. (3.1) are

$$\int ds' W \sigma K \longrightarrow R^{-2} \int ds' W \sigma K \Rightarrow \alpha = \frac{1}{3} \ , \tag{3.4}$$

$$\boldsymbol{\nabla}^2 K \longrightarrow R^{-3} \boldsymbol{\nabla}^2 K \Rightarrow \alpha = \frac{1}{4}, \tag{3.5}$$

$$\int ds' W Z \longrightarrow R^0 \int ds' W Z \Rightarrow \alpha = 1 \ , \tag{3.6}$$

$$\cos\theta K \longrightarrow R^{-1} \cos\theta K \Rightarrow \alpha = \frac{1}{2} \ . \tag{3.7}$$

These exponents characterize the power-law growth of the layer of accumulated material in the top and bottom of Fig. 1. The exponents $\alpha = \frac{1}{3}$ and $\alpha = 1$ are obtained from the term on the right-hand side of Eq. (A1) and they are related to fluxes across the bulk with an effective $(1 - a)$ diffusion coefficient. Furthermore, the exponents $\alpha = \frac{1}{4}$ and $\alpha = \frac{1}{2}$ are obtained from the second term on the left-hand side of Eq. (A1), and they are related

to fluxes along the interface, as indicated by the fact that the term in Eq. (A1) is only appreciably different from zero near the interface. The exponent $\alpha = \frac{1}{3}$ is the one obtained by Lifshitz-Slyosov theory. The exponent $\alpha = \frac{1}{4}$ was studied in detail in Ref. 14, and appears due to the presence of a concentration-dependent diffusion coefficient. The last two exponents, $\alpha = 1$ and $\alpha = \frac{1}{2}$, are generated by the presence of a gravitational field and are the ones on which we concentrate in the present study. The exponent $\alpha = 1$ corresponds to a simple linear growth as expected in a constant field. The most interesting exponent is $\alpha = \frac{1}{2}$. It takes into account the growth of a curved front due to the different gravitational energies associated with the different points on the front. For long enough times, we expect that only the $\alpha = 1$ and $\alpha = \frac{1}{2}$ exponents would be important, so we propose the following equation for the characteristic height $h(t)$:

$$\frac{dh(t)}{dt} = (1-a)C_1 + a\frac{C_2}{h(t)}. \tag{3.8}$$

We can define a critical height h_c as that for which the two contributions on Eq. (3.8) are equal. The fact that h_c is proportional to $a/(1-a)$ tells us that the linear growth will be dominant at longer times by increasing a. The crossover would occur at $t = 0$ for a=0 and at infinite time for a=1.

IV. NUMERICAL RESULTS

We have numerically integrated Eq. (2.4) in a two-dimensional lattice of size $L^2 = 120^2$ using Euler's method with mesh-size $\Delta x = 1$ and time step $\Delta t = 0.025$. We have considered rigid walls in the direction of the external field ($\hat{z}$) and periodic boundary conditions in the other direction ($\hat{x}$). The rigid walls are obtained by imposing zero flux at the points in positions $z = 1$ and $z = L$ (see Appendix B for details). The system is initially prepared by assigning to each point a uniformly random concentration in the interval (−0.05,0.05). The results have been averaged over 10 runs corresponding to different initial configurations. In Fig. 3 we present the final equilibrium profiles obtained by numerical integration of Eq. (2.4) for different values of the field g. It corresponds to the very long time evolution of the interface that appears at late stages in the evolution of Fig. 1. Furthermore, we also present the theoretical results given by Eq. (2.7) (Ref. 4) for the same values of g. The agreement is good for small values of g, as expected.

In Fig. 4 we present the results for the density-profile function, $C(z,t)$, which is defined by

$$C(z,t) = \frac{1}{L}\sum_{i=1}^{L} c[\mathbf{r} = (i,z),t]. \tag{4.1}$$

Since the process of accumulation is symmetric at the two walls we have averaged the results of both sides. For the same value of gravity g but decreasing the temperature (increasing a), we observe a slower evolution of the system to the same final configuration.

As a measure of the thickness of the front that is created by the accumulation of material at the walls, we introduce the length $h(t)$ defined as the first value of z that satisfies

$$| C[h(t),t] | = 0.5 \tag{4.2}$$

at each one of the walls. In Fig. 5, we show the evolution of $h(t)$ in a log-log plot for g=0.005 and four different values of the parameter a. We observe that the slope

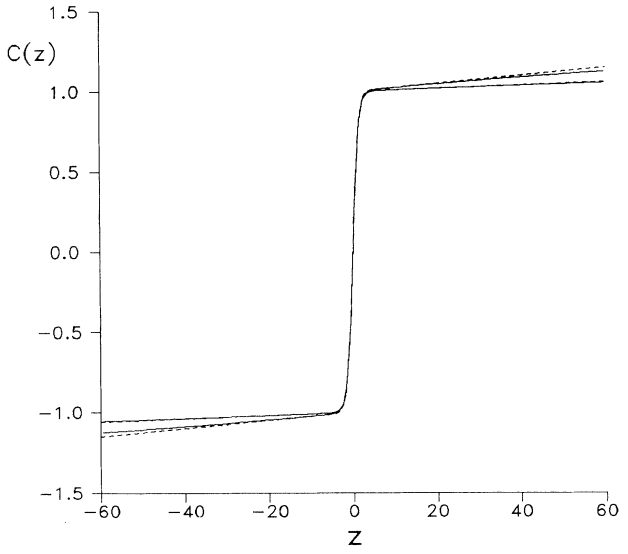

FIG. 3. Equilibrium profiles for gravitational fields g=0.001 and 0.005. The dashed lines show the theoretical approximation given by Eqs. (2.7)–(2.9) and the solid lines are the profiles obtained by numerical integration of Eq. (2.4) with a=0.

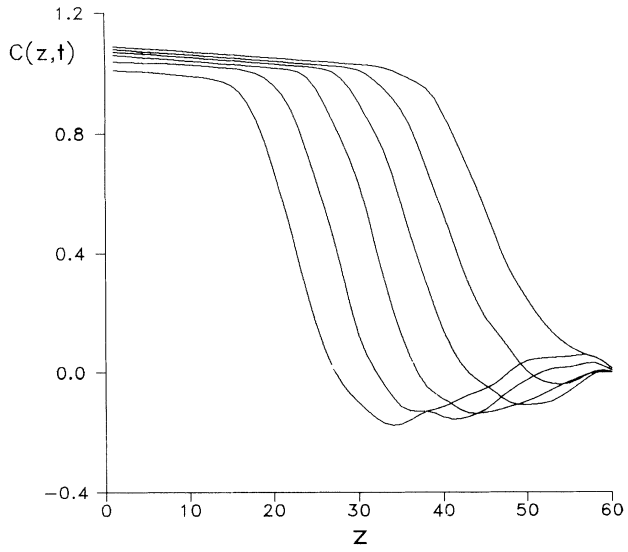

FIG. 4. Density-profile function [Eq. (4.1)] for g=0.005 and a=0 at times t=8000, 10 000, 12 000, 14 000, 16 000, and 18 000. The functions have been averaged at both layers.

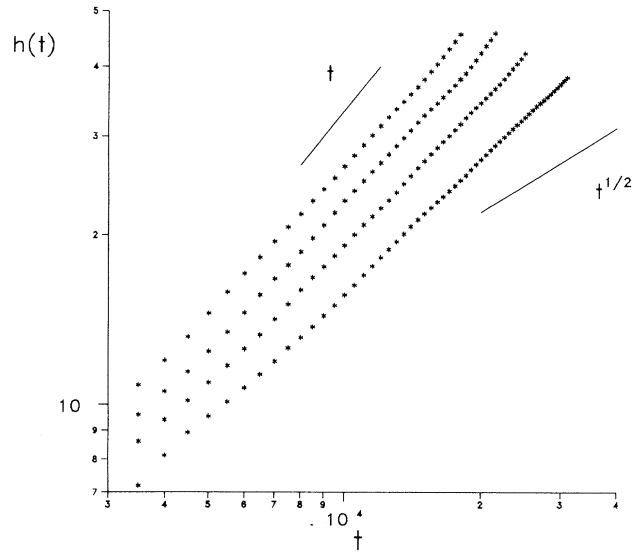

FIG. 5. log-log plot of the thickness of the front of accumulated material, $h(t)$, for g=0.005 and four different values of a: 0, 0.2, 0.4, and 0.6. The slower dynamics correspond to higher values of a. Solid lines represent $\alpha = 1$ and $\alpha = 1/2$ growth exponents.

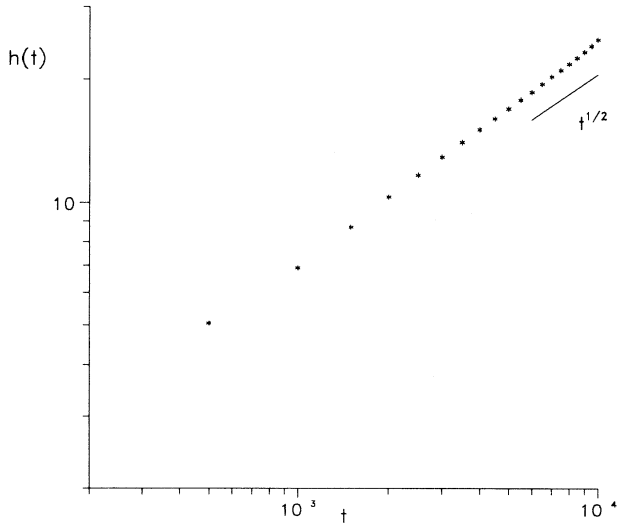

FIG. 6. log-log plot of the thickness of the front of accumulated material, for $g = 0.05$ and $a = 1$. See the text for details about the procedure of integration for this particular value. The solid line corresponds to the $\alpha = \frac{1}{2}$ growth exponent.

decreases as a is increased. In order to quantify this, we present in Table I the results for an effective exponent n obtained from a nonlinear fit of the form $h(t) = A + Bt^n$.[14] The numerical results for the evolution of $h(t)$ are in good qualitative agreement with the theoretical analysis of the previous section. We observe a smaller exponent for larger values of a. But the final evolution is characterized by an exponent $\alpha = 1$. However, in this model it is difficult to observe the presence of the $\alpha = \frac{1}{2}$ exponent and the predicted crossover. In fact, an estimation of the critical heights h_c (Table I) tell us that for all values in Fig. 5, $h(t) > h_c$, and the crossover has already occurred. The value of h_c can be obtained from the numerical data by a linear fit of Eq. (3.8). However, the errors involved in the numerical calculation of the derivative of $h(t)$ are very large, so we have estimated h_c by solving the differential equation (3.8) and fitted the data by minimizing the χ^2 function.

To determine the $\alpha = \frac{1}{2}$ growth in a more transparent way, we integrate numerically Eq. (2.4) for zero temperature ($a = 1$). To avoid the problem of a negative diffusion coefficient near the walls we take zero flux for $c > 1$. In Fig. 6 we show a log-log plot of the numerical results obtained for $h(t)$. We obtain a good quantitative agreement with the theory.

We have also performed simulations of Eq. (2.4) for both fixed and periodic boundary conditions to characterize the domain growth in the bulk. Our results are in agreement with a growth of the characteristic length of the domain in the direction of the gravitational field in the form $R \sim t^\alpha$ with $\alpha = 1$ in the long time behavior for $a \neq 0$ in accordance with Refs. 5 and 6. Furthermore, we also obtain $\alpha = \frac{1}{2}$ for $a = 1$. These results give an indication that the mechanism involved in the domain growth is similar to that of the front growth.

As the final remark of this section, we wish to point out that the approach presented here could be applied to a very general type of potential. In particular, the results of the numerical simulations presented in Ref. 8 in which the $\frac{1}{3}$ exponent is dominant could be understood by considering a similar theoretical analysis. In those cases, our scaling analysis predicts that the growth exponents are $\alpha = \frac{1}{3}$ or smaller.

TABLE I. Effective exponents n obtained for a fit of $h(t) = A + Bt^n$ and critical heights h_c, for g=0.005 and the same four values of a shown in Fig. 5.

a	n	h_c
0.0	0.95 ± 0.01	0
0.2	0.94 ± 0.01	2.3 ± 0.4
0.4	0.93 ± 0.01	3.7 ± 0.5
0.6	0.86 ± 0.01	5.5 ± 0.7

V. CONCLUSIONS AND COMMENTS

We have studied a model of spinodal decomposition in a gravitational field. The presence of a concentration-dependent diffusion coefficient is required for a proper treatment of gravity at the level of the dynamic equation. We have derived the corresponding interfacial equation by means of Green function techniques. By scaling arguments, we have derived the exponents of the different power-law behavior associated with the different mechanisms present in the front growth. Gravity induces a front of accumulation of material from the walls. This growth could be described by a power law which includes both bulk and interfacial diffusion mechanisms.

A crossover from interfacial to bulk exponents appears at later times for lower temperature and at infinite time for zero temperature. We have also studied this problem numerically with fixed and periodic boundary conditions to analyze both front and domain growth. The results are in good agreement with the theoretical predictions and indicate a similar growth mechanism for both. Our results could help in the explanation of the experimental results and we consider that the analysis in terms of interfacial equations is a powerful tool in the study of front and domain growth.

ACKNOWLEDGMENT

We acknowledge financial support of the Dirección General de Investigación Científica y Técnica (Spain) Project No. PB90-0030.

APPENDIX A: INTERFACIAL EQUATION

In order to derive an equation for the evolution of the front associated with the accumulation of material on the walls induced by the gravitational field, we introduce a system of curvilinear coordinates (u, s) such that s follows the contour of the interface and u goes along the normal direction of it, $\hat{n}(s)$, taking the value $u=0$ at the center of the interface. We write Eq. (2.4) as

$$\frac{\partial c}{\partial t} - a\nabla(1-c^2)\cdot\nabla\left(-\nabla^2 + \frac{\delta f(c)}{\delta c}\right) = (1-a)\nabla^2\left(-\nabla^2 c + \frac{\delta f(c)}{\delta c}\right) \quad \text{(A1)}$$

with

$$\frac{\delta f(c)}{\delta c} = -c + c^3 + g[Z(s) + u\cos\theta(s)], \quad \text{(A2)}$$

where $Z(s)$ is the position of the front in the $\hat{z}$ direction and $\theta(s)$ is the angle between $\hat{n}(s)$ and the direction of the external field $\hat{z}$.

We assume that at the normal direction, the profile is approximately the equilibrium profile for a flat interface, so that we separate $c(\mathbf{r}, t)$ in two terms:

$$c(\mathbf{r}, t) = c_{st}(u) + \delta c(\mathbf{r}, t), \quad \text{(A3)}$$

where $c_{st}(u)$ is the unidimensional equilibrium solution given by Eqs. (2.7)–(2.9), and δc is the deviation with respect to this solution. If we keep terms only to first order in δc and first order in the curvature K, defined as

$$K(s) = -\frac{d\theta(s)}{ds}, \quad \text{(A4)}$$

we can write

$$\nabla^2 c + \frac{\delta f}{\delta c} = -K(s)\frac{dc_{st}}{du} + gZ(s) + \left(\frac{\delta^2 f}{\delta c_{st}^2} - \nabla^2\right)\delta c. \quad \text{(A5)}$$

Assuming that δc does not depend on time (quasistatic approximation) and introducing the normal velocity

$$v(\mathbf{r}, t) = -\frac{\partial u(\mathbf{r}, t)}{\partial t}, \quad \text{(A6)}$$

Eq. (A1) can be written as

$$-v\frac{\partial c_{st}}{\partial u} - (1-a)\nabla^2\left(-K\frac{dc_{st}}{du} + gZ\right) = a\nabla(1-c_{st}^2)\cdot\nabla\left(-K\frac{dc_{st}}{du} + gZ\right) + L\delta c \quad \text{(A7)}$$

with the operator

$$L = \nabla(1-ac_{st}^2)\cdot\nabla\left(\frac{\delta^2}{\delta c_{st}^2} - \nabla^2\right) - 2agc_{st}\sin\theta(s)\frac{\partial}{\partial s}. \quad \text{(A8)}$$

By multiplying Eq. (A7) by the Green function defined by

$$\nabla^2 G(\mathbf{r}, \mathbf{r}') = \delta(\mathbf{r} - \mathbf{r}') \quad \text{(A9)}$$

and by dc_{st}/du, and integrating over u, u', and s', we obtain in the limit of thin interface that

$$4\int ds' G[\mathbf{r}(s), \mathbf{r}(s')]\left[v(s', t) - a\nabla^2 K(s') + ag\cos\theta(s')K(s')\right] = (1-a)\left[\sigma K(s) + 2gZ(s)\right], \quad \text{(A10)}$$

where σ is the surface tension

$$\sigma = \int_{-\infty}^{\infty} du\left[\frac{dc_{st}(u)}{du}\right]^2 \sim \frac{2\sqrt{2}}{3} + 2g. \quad \text{(A11)}$$

Now, using the inverse $W(\mathbf{r}, \mathbf{r}')$ of the Green function, we recover Eq. (3.1). In order to derive Eq. (A10) we have discarded the contribution which comes from the last term in Eq. (A8) when it operates over δc. We have considered that this term is very small due to the presence of δc, g, and $\sin\theta(s)$, which are small quantities in our approach.

APPENDIX B: NUMERICAL DETAILS OF THE BOUNDARY CONDITIONS

Here we present the numerical details used in our integration of Eq. (2.4), in order to implement the correct boundary conditions at the top and bottom of the sys-

tem. Equation (2.4) can be written as

$$\frac{\partial c}{\partial t} = \nabla \cdot \mathbf{J}(c), \tag{B1}$$

where the flux $\mathbf{J}(c)$ is given by

$$\mathbf{J}(c) = (1 - ac^2)\nabla(-c + c^3 - \nabla^2 c - gz). \tag{B2}$$

Equation (B1) is discretized as

$$\frac{\partial c}{\partial t} = \frac{1}{2}[\nabla^L J^R(c) + \nabla^R J^L(c)], \tag{B3}$$

where ∇^L and ∇^R are the left and right gradient operators.[18] J^L and J^R are given by Eq. (B2) where ∇ are ∇^L and ∇^R, respectively.

Due to the fact that $c(\mathbf{r}, t)$ is a conserved field we must impose the condition that the normal component of $\mathbf{J}$ at the boundaries (top and bottom) should be

$$J_z[c(1)] = J_z[c(L)] = 0. \tag{B4}$$

For the sake of simplicity we will present the explicit formulas for a one-dimensional model with reflecting boundaries in the cells $i = 1$ and $i = L$. The discrete version of Eq. (B3) is

$$\frac{\partial c_i}{\partial t} = \frac{1}{2\Delta X}[J_z^R(i) - J_z^R(i-1) + J_z^L(i+1) - J_z^L(i)]. \tag{B5}$$

In order to impose zero flux across the barrier at the bottom ($i = 1$) we must define that

$$J_z^R(0) = -J_z^L(1) \tag{B6}$$

and reciprocally at the top ($i = L$) we can write that

$$J_z^L(L+1) = -J_z^R(L). \tag{B7}$$

So the equation of motion for the cell $i = 1$ is

$$\frac{\partial c_1}{\partial t} = \frac{\Delta t}{2\Delta x}[J_z^R(1) + J_z^L(2)] \tag{B8}$$

and for the cell $i = L$

$$\frac{\partial c_L}{\partial t} = \frac{\Delta t}{2\Delta x}[-J_z^R(L-1) - J_z^L(L)]. \tag{B9}$$

Equation (B5) for $i = 2, ..., L-1$ and Eqs. (B8) and (B9) solve the numerical integration of Eq. (B1) with reflecting boundaries at $i = 1$ and $i = L$.

[1] J.D. Gunton, M. San Miguel, and P.S. Shani, in *Phase Transitions and Critical Phenomena*, edited by C. Domb and J.L. Lebowitz (Academic, New York, 1983), Vol. 8, p. 267.

[2] K. Kitahara, Y. Oono, and D. Jasnow, Mod. Phys. Lett. B **2**, 765 (1988).

[3] D. Jasnow, in *Far from Equilibrium*, edited by L. Garrido, Lectures Notes in Physics Vol. 319 (Springer-Verlag, Berlin, 1988).

[4] Y. Shiwa, Physica A **148**, 414 (1988).

[5] C. Yeung, T. Rogers, A. Hernández-Machado, and D. Jasnow, J. Stat. Phys. **548**, 1141 (1992).

[6] S. Puri, K. Binder, and S. Dattagupta, Phys. Rev. B **46**, 98 (1992).

[7] S. Puri and K. Binder, Phys. Rev. A **46**, R4487 (1992).

[8] G. Brown and A. Chakrabarti, Phys. Rev. A **46**, 4829 (1992).

[9] J.S. Langer, M. Bar-on, and H.D. Miller, Phys. Rev. A **11**, 1417 (1975).

[10] K. Kitahara and M. Imada, Prog. Theor. Phys. Suppl. **64**, 65 (1978).

[11] S. Puri and Y. Oono, Phys. Rev. A **38**, 1542 (1988).

[12] C. Yeung, Ph.D. thesis, University of Illinois, 1989 (unpublished).

[13] T. Ohta, J. Phys. C **21**, L361 (1988).

[14] A. Lacasta, A. Hernández-Machado, J.M. Sancho, and R. Toral, Phys. Rev. B **45**, 5276 (1992).

[15] A. Lacasta, J.M. Sancho, A. Hernández-Machado, and R. Toral, Phys. Rev. B **48**, 6854 (1993).

[16] K. Kawasaki and T. Ohta, Physica A **118**, 175 (1983).

[17] T. Rogers, Ph.D. thesis, University of Toronto, 1989 (unpublished).

[18] *Handbook of Mathematical Functions,* edited by M. Abramowitz and I. Stegun (Dover, New York, 1970).

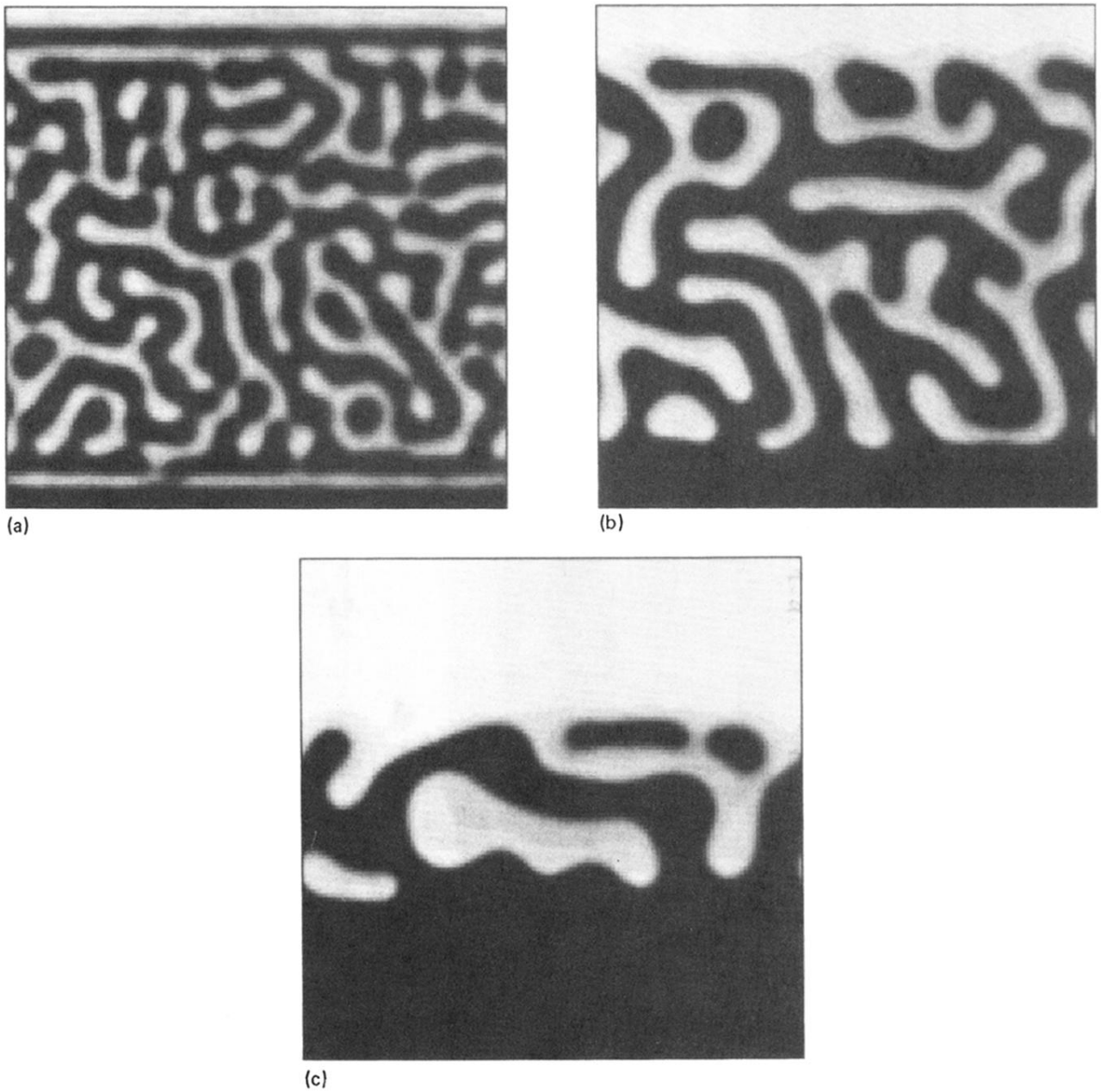

FIG. 1. Typical temporal evolution of phase separation for a critical quench in the presence of gravity, with $g = 0.1$ and $a = 0.8$. The figures correspond to the times (a) t=100, (b) t=500, and (c) t=2000.

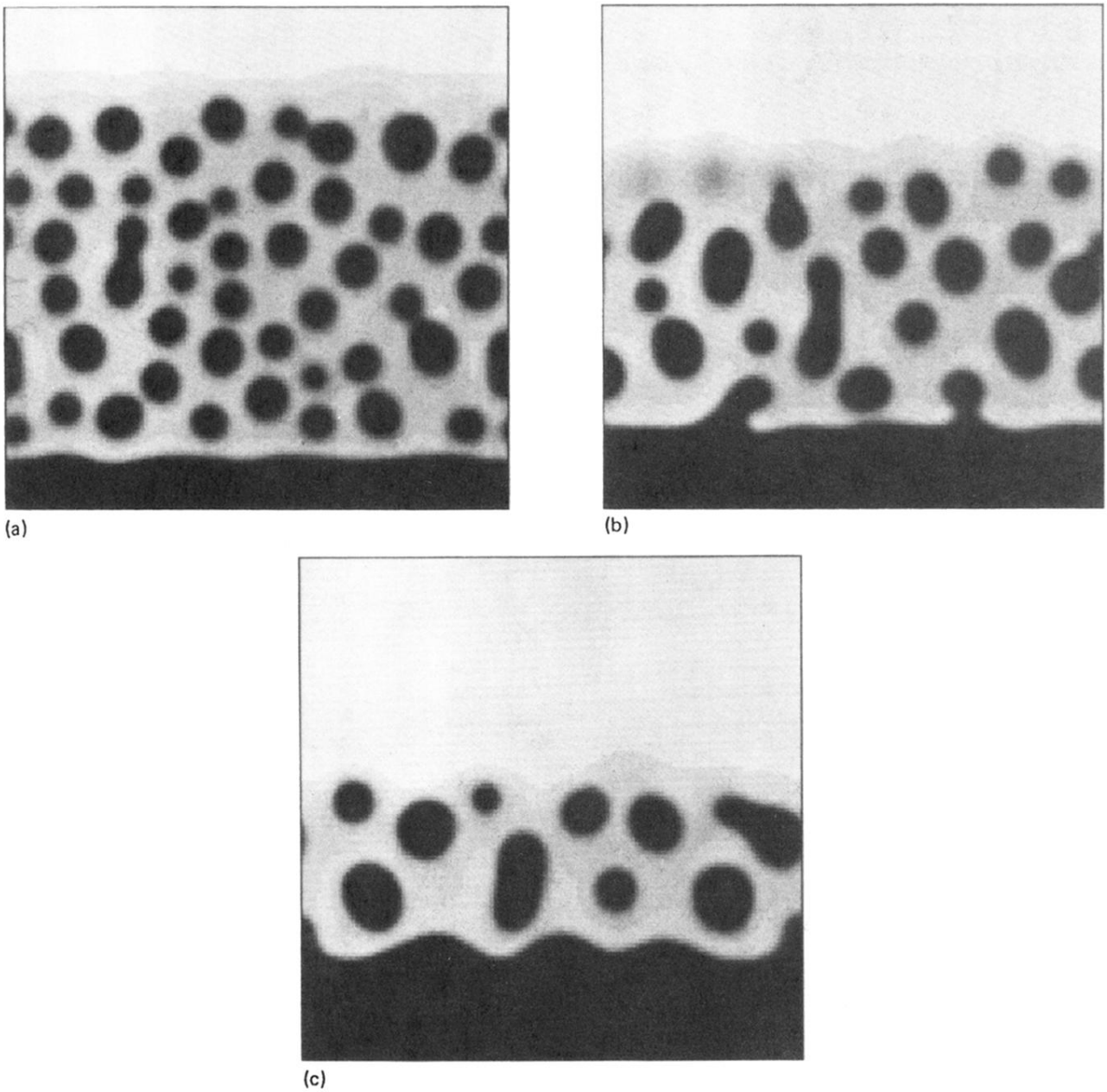

FIG. 2. Typical evolution for an off-critical quench that corresponds to a volume fraction of the minority phase $\phi = 30\%$, in the presence of gravity, with g=0.1 and a=0.8. The figures correspond to the times (a) t=500, (b) t=1000, and (c) t=1500.